On-Chip Quantum Interference from a Single Silicon Ring-Resonator Source

Stefan F. Preble,[1,*] Michael L. Fanto,[2] Jeffrey A. Steidle,[1] Christopher C. Tison,[2]
Gregory A. Howland,[2] Zihao Wang,[1] and Paul M. Alsing[2]

[1]*Rochester Institute of Technology, Microsystems Engineering, 168 Lomb Memorial Drive,
Rochester, New York 14623, USA*
[2]*Air Force Research Laboratory, 525 Brooks Road, Rome, New York 13441, USA*

Here we demonstrate quantum interference of photons on a silicon chip produced from a single-ring-resonator photon source. The source is seamlessly integrated with a Mach-Zehnder interferometer, which path entangles degenerate biphotons produced via spontaneous four-wave mixing in the silicon ring resonator. The resulting entangled N00N state is controlled by varying the relative phase of the integrated Mach-Zehnder interferometer, resulting in high two-photon interference visibilities of $V \sim 96\%$. Furthermore, we show that the interference can be produced using pump wavelengths tuned to all of the ring resonances accessible with our tunable lasers ($C + L$ band). This work is a key demonstration towards the simplified integration of multiple photon sources and quantum circuits together on a monolithic chip, in turn, enabling quantum-information chips with much greater complexity and functionality.

Introduction.—Silicon photonics is proving to be a promising platform for quantum-information processing applications [1–11]. Photon sources with high brightness and spectral purity, low noise, and compact footprints have been demonstrated using spontaneous four-wave mixing (SFWM) in ring or microdisk resonators [12–19]. These sources have been used to demonstrate time-energy entanglement in off-chip setups and photonic integrated circuits [3,20]. High-efficiency superconducting nanowire single-photon detectors have also been integrated with waveguide-based quantum circuits [4,21–24] enabling the integration of all of the key components of a quantum-information processor. However, complex quantum information processors will require many sources to be integrated and entangled together. Recently, steps have been taken towards this with the integration of photon sources and entanglement circuits on a single silicon chip [1,25]. However, these demonstrations require multiple independent photon sources to realize two-photon entanglement. *Ergo*, the inherent fabrication variations in the sources will yield photon pairs that are potentially distinguishable. These fabrication variations are alleviated partially in the case of resonant photon sources by using a pulsed pump laser, but it is advantageous to be able to make use of narrow-linewidth continuous-wave pump lasers in order to ensure long coherence lengths of the entangled photon states.

Device design.—Here we demonstrate the entanglement of photon pairs produced from a *single*-ring-resonator photon source. A single ring resonator ensures that the entangled photons will be indistinguishable since they are generated within the same device. Furthermore, since entanglement is realized from a single device, the number of photon-source devices in an entangling circuit can be halved. Furthermore, we show here that the resonant photon source can be operated with pump-laser wavelengths that span approximately 80 nm, in turn, enabling wavelength multiplexing in future systems. Consequently, this research is a key advance in the simplification of integrated quantum-information systems and will enable complex integration of sources and entanglement circuits together for a wide variety of quantum technologies such as quantum key distribution and possibly even quantum computation.

In order to use a single ring resonator as an entangled photon source, we excite the resonator bidirectionally. The excitation is seen in Fig. 1(a) where two pump lasers [pump 1 (blue) and pump 2 (red) each tuned to a resonance of the ring resonator] are launched into the silicon chip. On the chip, they are immediately split with a Y splitter [26] and routed into a loop. The counterpropagating pumps are then coupled into a ring-resonator photon source (radius $R = 18.5 \ \mu$m, waveguide dimensions of $W = 500$ nm by $H = 220$ nm, and a waveguide to ring gap of $g = 150$ nm) where they induce SFWM in opposite directions, which generates entangled photon pairs. The ring resonator is designed to have zero dispersion; therefore, when the pump frequencies are tuned to resonances that are equally spaced from a central resonance, degenerate biphotons are produced as dictated by the energy-conservation relation: $E_{\text{pump 1}} + E_{\text{pump 2}} = E_{\text{biphoton}}$ [depicted by the virtual energy-level diagram in Fig. 1(a)]. We have recently shown that this photon-generation process results in bright (approximately 3×10^5 photons/s mW² GHz) low-noise
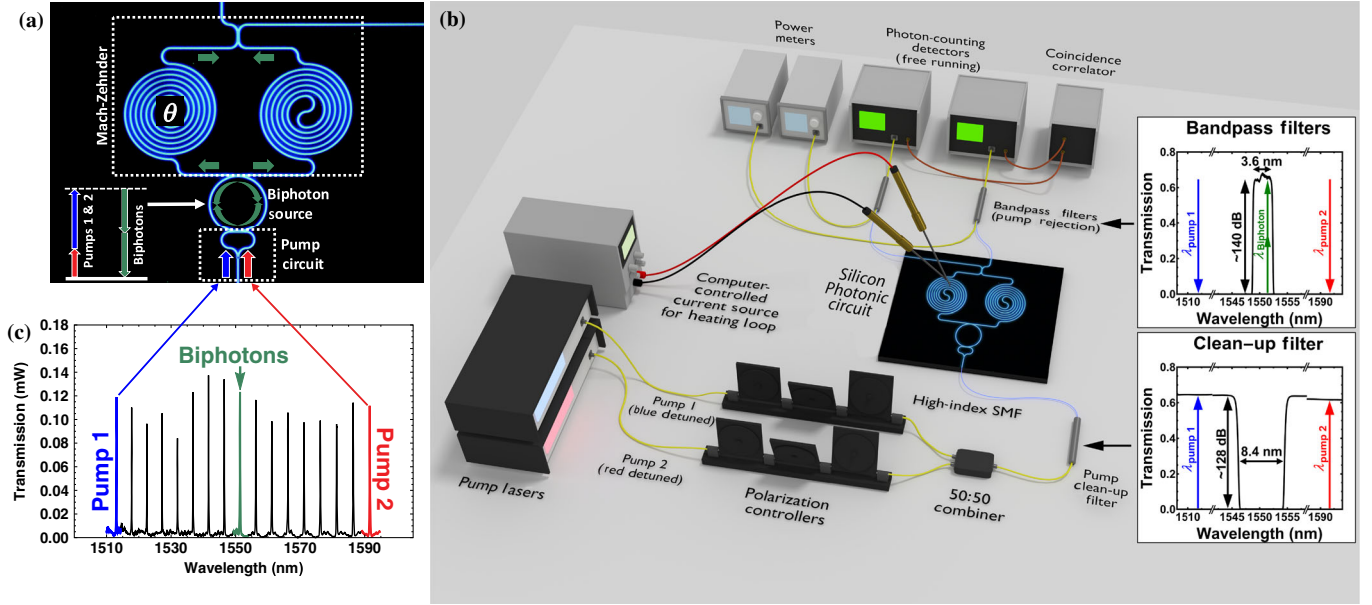
*Corresponding author.
Stefan.Preble@rit.edu

FIG. 1.   (a) Microscope image of the quantum circuit that consists of an integrated pump splitting circuit, ring resonator (Q of 15,000, FSR of 5 nm) entangled biphoton source and MZI analysis circuit. The devices were fabricated using e-beam lithography, with typical waveguide losses of 3 dB/cm [27]. (b) Schematic of the complete experimental setup. A pair of tunable lasers are polarized, combined and passed through pump clean-up filters. A short section of High Index fiber (Nufern UHNA-7) was spliced to optical fiber (SMF-28) to efficiently mode match to the Silicon waveguide achieving a total insertion loss of approximately 5 dB [16]. The relative phase (θ) in the MZI was controlled by thermal heating of one of the spirals. Photons from the two outputs were filtered to remove noise, the rejected pumps are sent to power meters to measure the classical signatures. The biphotons are detected by InGaAs APDs (idQuantique ID210 – 10% Efficiency, ID230 – 25% Efficiency) and correlated using a time-to-digital converter. (c) Transmission spectrum (when the MZI is tuned for 50/50 splitting) indicating the wavelengths of the two pump lasers as well as the wavelength of the resulting biphotons.

(ratio between coincidence counts and accidental-coincidence counts (CAR) of greater than 500), degenerate biphotons [16].

For this experiment, we set the generation rate to be sufficiently low so that higher-order generation events are unlikely to occur. In such a regime, we can approximate the state generated within the ring resonator to be

$$|\psi\rangle_{\mathrm{ring}} = \tfrac{1}{2}[\hat{a}_{\mathrm{cw}}^{\dagger\,2} + \hat{a}_{\mathrm{ccw}}^{\dagger\,2}]|\mathrm{vac}\rangle, \qquad (1)$$

where $\hat{a}_{\mathrm{cw}}^{\dagger}$ and $\hat{a}_{\mathrm{ccw}}^{\dagger}$ are independent creation operators for clockwise- and counterclockwise-propagating biphotons, respectively. This unique pumping configuration results in a two-photon N00N state ($N = 2$), which is a well-known form of entangled state that exhibits a factor of N sensitivity to relative phase changes over classical light.

This state is coupled out of the resonator and into a Mach-Zehnder Interferometer (MZI) analysis circuit for confirmation [Fig. 1(a)]. The circuit is composed of two spiraled waveguide legs (approximately 1 mm length). One of the spirals is thermally tuned to induce a relative phase shift (θ) between the two paths. Combining the legs of the MZI onto a 50:50 directional coupler completes the analysis resulting in the phase-dependent output state

$$|\psi\rangle_{\mathrm{out}} = \frac{1}{4} e^{-i\theta}[\hat{a}_{\mathrm{cw}}^{\dagger\,2} - \hat{a}_{\mathrm{ccw}}^{\dagger\,2} + 2i\hat{a}_{\mathrm{cw}}^{\dagger}\hat{a}_{\mathrm{ccw}}^{\dagger}$$
$$+ (-\hat{a}_{\mathrm{cw}}^{\dagger\,2} + \hat{a}_{\mathrm{ccw}}^{\dagger\,2} + 2i\hat{a}_{\mathrm{cw}}^{\dagger}\hat{a}_{\mathrm{ccw}}^{\dagger})e^{2i\theta}]|\mathrm{vac}\rangle. \quad (2)$$

This state oscillates between high coincidence and zero coincidence as a function of the phase delay as follows:

$$|\psi\rangle_{\mathrm{coinc}} = i\hat{a}_{\mathrm{cw}}^{\dagger}\hat{a}_{\mathrm{ccw}}^{\dagger}|\mathrm{vac}\rangle, \qquad \theta = \pi n, \qquad n = 0, 1, 2, \dots, \quad (3)$$

$$|\psi\rangle_{\mathrm{no\ coinc}} = \frac{i}{2}[\hat{a}_{\mathrm{cw}}^{\dagger\,2} - \hat{a}_{\mathrm{ccw}}^{\dagger\,2}]|\mathrm{vac}\rangle,$$
$$\theta = \pi(n + \tfrac{1}{2}), \qquad n = 0, 1, 2, \dots. \quad (4)$$

The distinguishing feature of this two-photon interference is that it oscillates at twice the frequency as classical light. Specifically, the biphotons interfere at the output of the MZI so that they either bunch together (no coincidences) or antibunch (coincidences) at phase shifts that are multiples of π, whereas classical light in the MZI experiences constructive or destructive interference over multiples of 2π.

Experimental results.—The difference in oscillation frequency is shown in Fig. 2 where the measured classical signal and coincidences are plotted. The classical light output from the two ports of the MZI is shown in Fig. 2(a). As the relative phase is changed, the signals cycle between
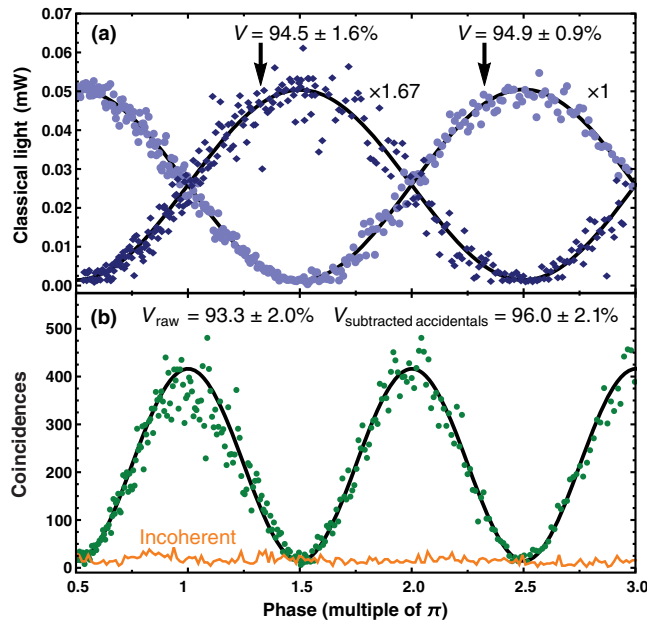
FIG. 2. (a) Classical laser light from the two outputs of the silicon circuit as varying the relative phase of the MZI. The heating power was converted to phase using a fit assuming the phase linearly depends on temperature. The blue- diamond data was scaled by a factor of ×1.67 for ease of comparison. This path experienced a higher loss on the chip because of fabrication imperfections. (b) Coincidences between the two paths measured for ninety-seconds. The coincidences were measured with a 32 ps time resolution and integrated over 224 ps in order to account for the timing jitter of the APDs. The accidentals were obtained by averaging the time correlations far away from the coincidence peak over a time interval of 320 ns. The calculated error is obtained from the standard deviation of the accidentals over the same range. (Incoherent): Coincidence counts when the pumps are tuned asymmetrically about the central resonance, resulting in independent, incoherent, photon pairs.

destructive and constructive interference, and it is clear that the coincidences shown in Fig. 2(b) oscillate at twice the frequency, supporting our theorized output state in Eq. (2).

In order to show that the two-photon interference is a direct result of the generation of an entangled biphoton quantum state in a single ring resonator, we shift the wavelength of the "pump 2" laser by one resonant peak towards the central biphoton resonance [seen in Fig. 1(c)]. In this case, energy conservation dictates that the generated biphotons will no longer be generated at the symmetrically centered resonance ($\lambda_{\text{biphoton}} \sim 1551$ nm). Instead, any biphotons that can be generated will have to be at a wavelength that does not correspond to an actual resonance, which strongly inhibits their generation [17]. We do note though that if any biphotons are to be generated, they will still fall within the transmission window given by the bandpass pump rejection filters [Fig. 1(b)], and, as a result, they will be measured. However, as is seen in Fig. 2(b) ("incoherent," orange line), no coincidences are observed,

and we conclude that entangled biphotons are not generated even though both pump lasers are still producing photons.

The observed photon interference in Fig. 2(b) has a measured visibility of $V_{\text{raw}} = 93.3 \pm 2.0\%$. When the accidental counts are subtracted (removing the noise from the detectors and other photon-generation processes [1]), the visibility is observed to be $V = 96.0 \pm 2.1\%$. These high visibilities indicate that the observed coincidences arise from the biphoton entanglement discussed in this Letter. We do note though that the visibilities can be improved upon. First, it is seen that the classically measured visibilities in Fig. 2(a) are lower than desired. This is likely due to unoptimized directional couplers (e.g., length and wave-guide separation gap) in the MZI. By analyzing the dependence of visibility on the directional coupler splitting ratio and by also using other test structures on the same chip, we believe the directional coupler in this device is within $\pm 7\%$ of a $50\!:\!50$ coupling ratio. In the future, we plan to integrate heaters and optimized directional coupler designs to mitigate this variation [28]. Another source of noise is seen in the coincidence data around a phase shift of approximately π. This noise is due to the thermal and mechanical stability of the setup, particularly, the electrical needle probes used to locally heat one leg of the MZI. Since the data are measured over many hours, the probes inevitably shift position, which strongly affects the coincidences at this point because they occur over the high-sensitivity quadrature points of the classical signal.

The peak coincidences observed are also limited by loss within the device and the detectors. The free-running InGaAs photon detectors have relatively low dark count rates (approximately 2.5 kHz for the ID210 and approximately 200 Hz for the ID230) when operated with long dead times (50 μs for the ID210 and 25 μs for the ID230). We characterized the detectors, and for the photon flux detected, we determine that approximately 50% of the photons are being lost within the dead time of the detector. Consequently, the actual coincidences can be increased by approximately 4 times with better detectors. It should also be noted that the ring-resonator photon-generation device itself has an effective photon-pair loss. Specifically, the biphotons generated within the microring cavity may be lost through different ports of the ring resonator, as recently pointed out by Vernon and Sipe in Ref. [29]. However, this is inherently true for any resonator that has intrinsic loss— even one that is just coupled to a single waveguide [29]. In contrast, the double-bus ring resonator used here enables the control of the relative coupling strengths and simplifies the integration of the source with the analysis circuit.

Noise is also produced by nondegenerate photons produced by the pumps acting independently of each other [16]. Therefore, each pump spontaneously produces an incoherent photon at the biphoton resonance. In order to minimize this effect, it is key to optimize the relative powers of the two pump lasers. Specifically, if the laser

powers are not matched, more nondegenerate photon pairs will be produced by the stronger pump. Consequently, matched pump powers maximizes the CAR of the biphotons. For all of the measurements shown in this Letter, this optimization is done and results in a CAR of 80 when both pumps each have 1 mW of power (350 uW each at the chip). We note that this CAR is lower than in our previous work [16] because here we had to use photon detectors with higher noise (approximately kilohertz vs hertz), traded off photon flux for a bit more noise, and the additional elements in the circuit yield more loss, which degrades performance. Regardless, higher CAR's can be obtained through further circuit optimization and at lower pump-power levels, but we select this power as it gives a reasonable trade-off between noise and photon flux. We also note that noise is produced from Raman processes in the UHNA7 fiber and the glass cladding surrounding the silicon waveguide [16].

While the presence of multiple resonance modes is a challenge from a noise standpoint, the multiple resonances provide flexibility in how the biphotons are produced, as long as energy conservation is met for the process and the dispersion remains flat. As shown in Fig. 3(a)–3(f) when the two pump lasers are symmetrically tuned to all resonances over a range spanning up to $\Delta\lambda = \lambda_2 - \lambda_1 = 78.5$ nm and down to $\Delta\lambda = 19.4$ [which is the closest the pumps can be placed together due to the limitations of the filter bandwidths; see Fig. 1(b) insets], high-visibility two-photon interference is observed. We note though that there are some variations in both the peak coincidences and the accidental counts that yield variability in the observed visibility. We believe the variation is due to the weak wavelength dependence observed for the entire circuit [Fig. 1(c)], which is likely a result of the dispersion of the directional couplers. Regardless, the ability to use any resonant wavelengths to produce the two-photon interference enables flexibility for future wavelength division multiplexed integrated quantum circuits.

Another important consideration is how selective the wavelength dependence of the two-photon interference is. We measure the spectral selectivity of the resonator by setting the relative phase of the MZI to π (i.e., peak coincidences) and then scan the wavelengths of both pump lasers, as seen in Figs. 3(g) and 3(h). We find that the coincidences occur only when the two pump wavelengths coincide with the energy-conservation relation of the spontaneous four-wave-mixing process. Here this corresponds to $\Delta\lambda_{\mathrm{FWHM}} \sim 0.13$ nm, which closely matches the inherent spectral width of the ring resonances and supports the conclusion that the biphoton bandwidth is dictated by the resonator [17].

Conclusion.—We have demonstrated quantum interference of photons produced from a single Silicon ring resonator photon source. Entanglement was achieved by exploiting the inherent degeneracy of the clockwise and counterclockwise modes of a ring resonator. This research effectively doubles the functionality of a single ring resonator photon source and will enable considerable simplification of future multiqubit entanglement quantum circuits that rely on multiple photon sources. Here a ring resonator with a relatively large radius was used in order to demonstrate wavelength flexibility of a resonant photon source, which traded off source brightness (approximately 1×10^5 photons/s/mW^2/GHz). However, in future work, the quality factor of the resonator can be engineered and/or a smaller diameter resonator could be used to increase source brightness and minimize non-degenerate photon noise.
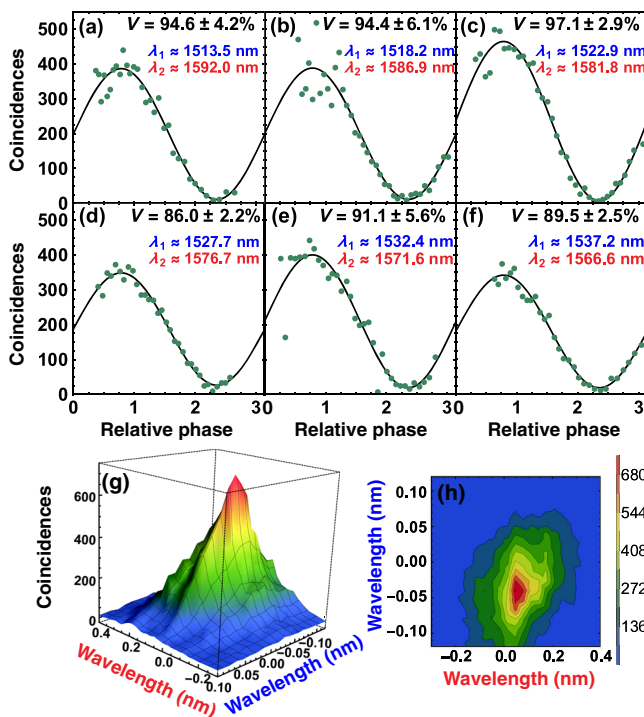

FIG. 3.   (a)–(f) Coincidences for different pump-laser wavelengths. (g),(h) Dependence of the coincidences on the wavelengths of the two pump lasers. The scales are different because the New Focus laser (blue scale with range −0.1 to 0.1 nm) has a very limited fine-tuning range.

[1] J. W. Silverstone, D. Bonneau, K. Ohira, N. Suzuki, H. Yoshida, N. Iizuka, M. Ezaki, C. M. Natarajan, M. G. Tanner, R. H. Hadfield, V. Zwiller, G. D. Marshall, J. G. Rarity, J. L. O'Brien, and M. G. Thompson, On-chip quantum interference between silicon photon-pair sources, Nat. Photonics **8**, 104 (2013).

[2] N. C. Harris, D. Grassani, A. Simbula, M. Pant, M. Galli, T. Baehr-jones, M. Hochberg, D. Englund, D. Bajoni, and

C. Galland, Integrated Source of Spectrally Filtered Correlated Photons for Large-Scale Quantum Photonic Systems, Phys. Rev. X, **4,** 041047(2014).

[3] D. Grassani, S. Azzini, M. Liscidini, M. Galli, M. J. Strain, M. Sorel, J. E. Sipe, and D. Bajoni, Micrometer-scale integrated silicon source of time-energy entangled photons, Optica **2,** 88 (2015).

[4] F. Najafi, J. Mower, N. C. Harris, F. Bellei, A. Dane, C. Lee, X. Hu, P. Kharel, F. Marsili, S. Assefa, K. K. Berggren, and D. Englund, Scalable integration of single-photon detectors, Nat. Commun. **6,** 5873 (2015).

[5] C. Schuck, W. H. P. Pernice, and H. X. Tang, Waveguide integrated low noise NbTiN nanowire single-photon detectors with milli-Hz dark count rate, Sci. Rep. **3,** 1893 (2013).

[6] N. Matsuda, P. Karkus, H. Nishi, T. Tsuchizawa, W. J. Munro, H. Takesue, and K. Yamada, On-chip generation and demultiplexing of quantum correlated photons using a silicon-silica monolithic photonic integration platform, Opt. Express **22,** 22831 (2014).

[7] X. Xu, Z. Xie, J. Zheng, J. Liang, T. Zhong, M. Yu, S. Kocaman, G.-Q. Lo, D.-L. Kwong, D. R. Englund, F. N. C. Wong, and C. W. Wong, Near-infrared Hong-Ou-Mandel interference on a silicon quantum photonic chip, Opt. Express **21,** 5014 (2013).

[8] K. Harada, H. Takesue, H. Fukuda, T. Tsuchizawa, T. Watanabe, K. Yamada, Y. Tokura, and S. Itabashi, Indistinguishable photon pair generation using two independent silicon wire waveguides, New J. Phys. **13,** 065005 (2011).

[9] M. Davanço, J. R. Ong, A. B. Shehata, A. Tosi, I. Agha, S. Assefa, F. Xia, W. M. J. Green, S. Mookherjea, and K. Srinivasan, Telecommunications-band heralded single photons from a silicon nanophotonic chip, Appl. Phys. Lett. **100,** 261104 (2012).

[10] A. Dutt, K. Luke, S. Manipatruni, A. L. Gaeta, P. Nussenzveig, and M. Lipson, On-Chip Optical Squeezing, Phys. Rev. Applied **3,** 044005 (2015).

[11] R. Kumar, J. R. Ong, M. Savanier, and S. Mookherjea, Controlling the spectrum of photons generated on a silicon nanophotonic chip, Nat. Commun. **5,** 5489 (2014).

[12] S. Azzini, D. Grassani, M. J. Strain, M. Sorel, L. G. Helt, J. E. Sipe, M. Liscidini, M. Galli, and D. Bajoni, Ultra-low power generation of twin photons in a compact silicon ring resonator, Opt. Express **20,** 23100 (2012).

[13] R. Wakabayashi, M. Fujiwara, K. Yoshino, Y. Nambu, M. Sasaki, and T. Aoki, Time-bin entangled photon pair generation from Si micro-ring resonator, Opt. Express **23,** 1103 (2015).

[14] E. Engin, D. Bonneau, C. M. Natarajan, A. S. Clark, M. G. Tanner, R. H. Hadfield, S. N. Dorenbos, V. Zwiller, K. Ohira, N. Suzuki, H. Yoshida, N. Iizuka, M. Ezaki, J. L. O'Brien, and M. G. Thompson, Photon pair generation in a silicon micro-ring resonator with reverse bias enhancement, Opt. Express **21,** 27826 (2013).

[15] S. Clemmen, K. P. Huy, W. Bogaerts, R. G. Baets, P. Emplit, and S. Massar, Continuous wave photon pair generation in silicon-on-insulator waveguides and ring resonators, Opt. Express **17,** 16558 (2009).

[16] J. A. Steidle, M. L. Fanto, C. C. Tison, Z. Wang, S. F. Preble, P. M. Alsing, High spectral purity silicon ring resonator photon-pair source, Proc. SPIE Int. Soc. Opt. Eng. **9500,** 950015 (2015).

[17] W. C. Jiang, X. Lu, J. Zhang, O. Painter, and Q. Lin, A silicon-chip source of bright photon-pair comb, arXiv:1210.4455v1.

[18] R. Kumar, J. R. Ong, J. Recchio, K. Srinivasan, and S. Mookherjea, Spectrally multiplexed and tunable-wavelength photon pairs at 1.55 μm from a silicon coupled-resonator optical waveguide, Opt. Lett. **38,** 2969 (2013).

[19] C. Reimer, L. Caspani, M. Clerici, M. Ferrera, M. Kues, M. Peccianti, A. Pasquazi, L. Razzari, B. E. Little, S. T. Chu, D. J. Moss, and R. Morandotti, CMOS-compatible, multiplexed source of heralded photon pairs: Towards integrated quantum combs, Opt. Express **22,** 6535 (2014).

[20] Y. Guo, W. Zhang, S. Dong, Y. Huang, and J. Peng, Telecom-band degenerate-frequency photon pair generation in silicon microring cavities, Opt. Lett. **39,** 2526 (2014).

[21] C. Schuck, W. H. P. Pernice, and H. X. Tang, Waveguide integrated low noise NbTiN nanowire single-photon detectors with milli-Hz dark count rate, Sci. Rep. **3,** 1893 (2013).

[22] F. Najafi, J. Mower, N. C. Harris, F. Bellei, A. Dane, C. Lee, X. Hu, P. Kharel, F. Marsili, S. Assefa, K. K. Berggren, and D. Englund, On-chip detection of non-classical light by scalable integration of single-photon detectors, Nat. Commun. **6,** 5873 (2015).

[23] S. Ferrari, O. Kahl, V. Kovalyuk, G. N. Goltsman, A. Korneev, and W. H. P. Pernice, Waveguide-integrated single- and multi-photon detection at telecom wavelengths using superconducting nanowires, Appl. Phys. Lett. **106,** 151101 (2015).

[24] A. Beyer, R. Briggs, F. Marsili, J. D. Cohen, S. M. Meenehan, O. J. Painter, and M. Shaw, in *Proceedings of CLEO 2015* (OSA, Washington, DC, 2015), p. STh1I.2.

[25] J. W. Silverstone, R. Santagati, D. Bonneau, M. J. Strain, M. Sorel, J. L. O. Brien, and M. G. Thompson, Qubit entanglement on a silicon photonic chip, arXiv:1410.8332v4.

[26] Y. Zhang, S. Yang, A. E.-J. Lim, G.-Q. Lo, C. Galland, T. Baehr-Jones, and M. Hochberg, A compact and low loss *Y*-junction for submicron silicon waveguide, Opt. Express **21,** 1310 (2013).

[27] L. Cao, A. A. Aboketaf, and S. F. Preble, CMOS compatible micro-oven heater for efficient thermal control of silicon photonic devices, Opt. Commun. **305,** 66 (2013).

[28] J. Van Campenhout, W. M. J. Green, S. Assefa, and Y. A. Vlasov, Low-power, 2×2 silicon electro-optic switch with 110-nm bandwidth for broadband reconfigurable optical networks, Opt. Express **17,** 24020 (2009).

[29] Z. Vernon and J. E. Sipe, Spontaneous four-wave mixing in lossy microring resonators, Phys. Rev. A **91,** 053802 (2015).